ELSEVIER

Biochemical Pharmacology 63 (2002) 305–320

Biochemical Pharmacology

The involvement of L-γ-glutamyl-L-cysteinyl-glycine (glutathione/GSH) in the mechanism of redox signaling mediating MAPK^{p38}-dependent regulation of pro-inflammatory cytokine production

John J. Haddad*

Neuroscience Research Laboratory, Department of Anesthesia and Perioperative Care, University of California Medical Center, San Fransisco, CA 94143, USA

Received 19 July 2001; accepted 25 October 2001

Abstract

Redox regulation of mitogen-activated protein kinase (MAPK^{p38})-mediated pro-inflammatory cytokine production is not well characterized in the alveolar epithelium. It was hypothesized that the involvement of the MAPK^{p38} pathway in regulating lipopolysaccharide (LPS)-induced tumor necrosis factor (TNF)-α and interleukin-6 secretion is redox-sensitive and affected by NAC, an antioxidant and a precursor of glutathione, and L-buthionine-(*S,R*)-sulfoximine, an irreversible inhibitor of γ-glutamylcysteine synthetase, the rate-limiting enzyme in GSH biosynthesis. Exposure of fetal alveolar type II epithelial cells to *Escherichia coli*-derived LPS induced, in a time-dependent manner, the phosphorylation/activation of MAPK^{p38} (peak at 15 min). In addition, LPS up-regulated the phosphorylation of MAPK^{p38} in a dose-dependent manner. The effect of LPS on the MAPK^{p38} pathway was associated with the activation of MAPK-activated protein kinase, which phosphorylated the small 27 kDa heat-shock protein (Hsp27). LPS induced the phosphorylation of Hsp27 in a time- and dose-dependent manner. Selective blockage of the MAPK^{p38} pathway by a pyridinyl-imidazole (SB-203580) abrogated LPS-induced release of TNF-α and IL-6. Pre-treatment with NAC reduced LPS-mediated secretion of TNF-α and IL-6. Incubation of cells with NAC induced intracellular accumulation of GSH, but reduced the concentration of GSSG. On the other hand, pre-treatment with BSO augmented LPS-mediated secretion of TNF-α and IL-6. In addition, BSO induced intracellular accumulation of GSSG, but reduced the concentration of GSH. Whereas NAC blocked the phosphorylation/activation of MAPK^{p38}, BSO amplified the LPS-mediated effect on MAPK^{p38}. These results indicated that intracellular redox signaling plays an important role in regulating LPS-induced activation of the MAPK^{p38} pathway and MAPK^{p38}-mediated regulation of LPS-dependent inflammatory cytokine production in the alveolar epithelium.

Keywords: Antioxidant; Cytokines; Immunopharmacology; Pathophysiology; p38 MAPK; Redox

* Tel.: +1-415-476-8984; fax: +1-415-476-8841.
E-mail address: jhaddad@itsa.ucsf.edu (J.J. Haddad).

Abbreviations: NAC, *N*-acetyl-L-cysteine; ANOVA, analysis of variance; ARE, AU-rich element; BSA, bovine serum albumin; BSO, L-buthionine-(*S,R*)-sulfoximine; DTT, dithiothreitol; DMEM, Dulbecco's modified Eagle medium; DMSO, dimethyl sulfoxide; ELISA, enzyme-linked immunosorbent assay; ERK, extracellular signal-regulated kinase; fATII, fetal alveolar type II; FCS, fetal calf serum; GSH, L-γ-glutamyl-L-cysteinyl-glycine; HBSS, Hanks' balanced salt solution; Hsp27, heat-shock protein 27; HRP, horseradish peroxidase; H_2O_2, hydrogen peroxide; $^{\bullet}OH$, hydroxyl radical; IκB, inhibitory-κB; IKK, IκB kinase; IL, interleukin; LPS, lipopolysaccharide; LBP, lipopolysaccharide-binding protein; MKK, MAPK kinase; MAPK, mitogen-activated protein kinase; MAPKK, MAPK kinase; NF-κB, nuclear factor-κB; NIK, NF-κB inducing kinase; GSSG, oxidized glutathione disulfide; PBS, phosphate buffered saline; PGE_2, prostaglandin-E_2; Redox, reduction–oxidation; ROS, reactive oxygen species; RK, reactivating kinase; SDS-PAGE, sodiumdodecyl sulfate-polyacrylamide gel electrophoresis; SAPK, stress-activated protein kinase; $O_2^{\bullet -}$, superoxide anion; TMB, 3,3′,5,5′-tetramethylbenzidine dihydrochloride; TRX, thioredoxin; Thr, threonine; Tyr, tyrosine; TNF-α, tumor necrosis factor-α.

1. Introduction

Many extracellular stimuli, including pro-inflammatory cytokines and other inflammatory mediators [1], elicit specific cellular responses through the activation of MAPK signaling pathways [2]. MAPKs are a proline-targeted serine-threonine kinases that transduce environmental stimuli to the nucleus and they themselves are activated by upstream MAPK kinases (MAPKKs) on both threonine (Thr) and tyrosine (Tyr) residues within an 'activation loop' [2,3]. Once activated, MAPKs can phosphorylate and activate other kinases or nuclear proteins, including potential transcription factors and substrates [2–4]. The novel mammalian reactivating protein kinase (p38/RK) MAPKs are stress-activated protein kinases (SAPKs) that mediate responses to cellular stresses such as UV irradiation, osmotic imbalance, heat shock, DNA damage, bacterial products

0006-2952/02/$ – see front matter
PII: S0006-2952(01)00870-X

such as lipopolysaccharide-endotoxin, and inflammatory signals [5,6]. Furthermore, inflammatory mediators, such as cytokines, including interleukin (IL)-6 and TNF-α, activate p38/RK MAPK pathway in several cell types [2,3,7,8]. Of note, p38/RK MAP kinase has been recently implicated in regulating pro-inflammatory cytokine biosynthesis [5] and transcription [9].

The tripeptide L-γ-glutamyl-L-cysteinyl-glycine or glutathione (GSH), a ubiquitous thiol, plays a major role in maintaining intracellular reduction–oxidation (redox) equilibrium in the lung [10–15]. The cysteinyl moiety of GSH provides the reactive thiol as a functional element responsible for the diverse properties of glutathione, including (i) an antioxidant potential mediated by the peroxidase coupled reaction, (ii) regulation of cellular sulfhydryl status and redox equilibrium, (iii) governing pathways in neuroimmune–endocrine interactions as an immunopharmacological thiol, and (iv) regulation of the expression/activation of redox-sensitive transcription factors induced by stress-evoked responses [11,14,16]. The pivotal role of redox cycle in maintaining the integrity of the biological system in the face of oxidative stress and other challenges is, therefore, of particular clinical relevance. The immunopharmacological potential assigned to glutathione [16,17], furthermore, stems from established observations. IL-1 induced responses in mesangial cells, for instance, occurred through modulating redox equilibrium [18]. In addition, reactive oxygen species (ROS) signaling regulating the transcription of IL-4 [19], IL-6, IL-8 [20] and TNF-α [20,21] was mediated through a thiol-dependent mechanism. Interestingly, antioxidants [22–25] and glutathione precursors [19,20,26,27] have been shown to down-regulate cytokine synthesis, activation and downstream processes. In this respect, *N*-acetyl-L-cysteine (NAC), an antioxidant and a GSH precursor [14,28], has been shown to ameliorate cytokine transcription and synthesis [22,29,30], in addition to suppressing ROS-mediated lung injury [28]. In contrast, irreversible inhibition of γ-glutamylcysteine synthetase (γ-GCS), the rate-limiting enzyme in GSH biosynthesis, by the action of L-buthionine-(*S,R*)-sulfoximine (BSO) [14,31], has been shown to enhance cytokine release by inducing the intracellular accumulation of ROS [20,25,26].

Redox regulation of p38/RK-mediated pro-inflammatory cytokine transcription and biosynthesis has not been well characterized. It has been previously shown that thioredoxin (TRX), a redox control protein, negatively regulated p38/RK MAP kinase activation and p38 MAPK-mediated IL-6 expression [32,33]. In addition, Hashimoto *et al.* [30] recently reported that NAC attenuated TNF-α-induced p38/RK MAPK activation and the downstream IL-8-dependent pathway. One mechanism involved in the generation of ROS in a variety of cells is the oxidative burst, a process catalyzed by the multicomplex enzyme NADPH oxidase; p38/RK MAPK has been implicated to regulate this complex and subsequently couple intracellular redox signaling with the oxidative burst-dependent regulation of pro-inflammatory signals [34–36]. However, redox regulation of LPS-induced p38/RK MAPK-mediated pro-inflammatory cytokine biosynthesis in the alveolar epithelium has yet to be ascertained. Therefore, the aim of the present study was to investigate the role that glutathione and glutathione modulating agents play in mediating p38/RK kinase phosphorylation/activation, and to determine whether modulating redox equilibrium is involved in p38/RK-dependent regulation of inflammatory cytokines.

2. Materials and methods

2.1. Chemicals and reagents

Unless otherwise indicated, chemicals of the highest analytical grade were purchased from Sigma–Aldrich. The pyridinyl-imidazole SmithKline Beecham [(SB)-203580], a specific inhibitor of p38/RK MAPK [5], was obtained from Calbiochem-Novabiochem; SB-203580 was reconstituted in dimethyl sulfoxide (DMSO), where the final concentration of DMSO was determined to be $\leq$0.01%. Phospho-p38/RK MAPK (Thr180/Tyr182) and p38/RK MAPK antibodies were purchased from New England Biolabs Incorporation. Recombinant human heat-shock protein 27 (Hsp27) was obtained from Calbiochem-Novabiochem and kept stored at -70°.

2.2. Primary cultures of alveolar epithelia

Fetal alveolar type II (fATII) epithelial cells were isolated from lungs of fetuses, essentially as reported elsewhere [13,14,37]. Briefly, fetal rats were removed from pregnant Sprague–Dawley rats by cesarean section at day 19 of gestation (term = 22 days), the lungs excised, teased free from heart and upper airway tissue, and were finely minced then washed free of erythrocytes using sterile, chilled Mg^{2+}- and Ca^{2+}-free Hanks' balanced salt solution (HBSS; 0.5 mL per fetus). The cleaned lung tissue was re-suspended in 1 mL per fetus HBSS containing trypsin (0.1 mg/mL), collagenase (0.06 mg/mL) and DNase I (0.012%, w/v), and was agitated at 37° for 20 min. The solution was then centrifuged at 100 *g* for 2 min to remove undispersed tissue, the supernatant was saved to a fresh sterile tube and an equal volume of Dulbecco's modified Eagle medium (DMEM) with 10% (v/v) fetal calf serum (FCS) was added to the supernatant. After passing the supernatant through a 120 μm pore sterile mesh, the filtrate was centrifuged at 420 *g* for 5 min, the pellet re-suspended in 20 mL DMEM/FCS and the cells were placed into a T-150 culture flask for 1 hr at 37° to enable fibroblasts and non-epithelial cells to adhere. Unattached cells were washed three times by centrifugation at 420 *g* for 5 min each and then seeded onto 24 mm diameter Transwell-clear permeable supports (Costar; 0.4 μm pore size) at a density

of 5×10^6 cells per filter and were allowed to adhere overnight at 152 Torr (≈21% O_2/5% CO_2). DMEM/FCS was exchanged for 4 mL of serum-free PC-1 media (Biowhittaker), pre-equilibrated to $pO_2 = 152$ Torr and 37° 24 hr later and cells were maintained at this pO_2 until the experiment. In each case, and under conditions of independent pre-treatments, the adenylate energy charge, an index of cell viability and competence, remained ≥0.7 and transepithelial monolayer resistance was monitored constantly at 250–350 Ω cm^2 or more [13,14].

2.3. Drug treatment and measurement of pro-inflammatory cytokines by ELISA

Epithelial cells were pre-treated for 2 hr with either NAC (1–50 mM) or BSO (1–100 μM), washed twice in pre-equilibrated PC-1 medium and subsequently challenged with LPS (1 μg/mL) for 24 hr (LPS was derived from *E. coli*, serotype 026:B6). Cell-free supernatants were assayed for pro-inflammatory (R&D Systems, UK) cytokine release by two-site, solid phase, sandwich enzyme-linked immunosorbent assay (ELISA), essentially as recounted previously [25,26,38]. Briefly, rabbit immunoaffinity purified polyclonal anti-rat IL-6 (2 μg/mL) and TNF-α (2 μg/mL) antibodies were used to coat high-binding microtitre plates (MaxiSorp) in bicarbonate buffer (0.1 M $NaHCO_3$ and 0.1 M NaCl, pH 8.2) [25,26,39]. After blocking in 3% bovine serum albumin (BSA), recombinant (standard) and biotinylated (recognition) immunoaffinity purified sheep anti-rat cytokine antibodies were employed for secondary detection. The color was developed using streptavidin–poly-horseradish peroxidase (HRP) (Amersham Life Sciences) coupled with 3,3′,5,5′-tetramethylbenzidine dihydrochloride (TMB) and 1 mM H_2O_2. The optical density was read at 450 nm against a background filter measuring at 595 nm, where the inter- and intra-assay coefficients of variations were reported at ≤10%. Results were extracted from the linear regression of the positive slope and cytokine concentration was expressed in pg/mL.

2.4. Measurement of intracellular levels of reduced (GSH) and oxidized (GSSG) glutathione

Following treatments, reduced (GSH) glutathione concentrations were determined spectrophotometrically [13,14] in neutralized perchloric acid (PCA; 7%) extracts by following the glyoxylase-catalyzed production of *S*-lactyl-GSH at 240 nm in a 1 mL volume containing 790 μL phosphate buffer (25 mM KH_2PO_4; 25 mM K_2HPO_4; pH 6.8), 150 μL 1% BSA, 10 μL sample, 10 μL glyoxylase-I (1 mg/mL), and 40 μL methylglyoxal (0.1 M). Oxidized glutathione disulfide (GSSG) was determined in the same cuvette by addition of 1 mg/mL glutathione reductase and 8 μL of 12 mM β-NADPH and then by following the change in absorbance at 340 nm [13,14]. Drift inherent to the assay was controlled by subtracting the absorbance change observed over the same time period from control cuvettes containing the same reaction components but with a matched sample volume of deionized water. Protein content of each PCA precipitate was redissolved in 1 M NaOH and determined enabling results to be expressed as μmol/mg protein.

2.5. Preparation of subcellular extracts for Western analysis of p38 MAP kinase activation/phosphorylation

2.5.1. Analysis of p38/RK phosphorylation

Total protein extraction was performed by homogenizing primary cell tissue in a suitable volume of a buffer (1:40, w/v) containing 20 mM HEPES (pH 7.5), 1.5 mM $MgCl_2$, 0.2 mM EDTA and 0.1 M NaCl [13,14]. Before extraction 5 mM dithiothreitol (DTT), 1 mM phenylmethylsulfonyl fluoride (PMSF), and 1.2 mM sodium orthovanadate (Na_3VO_4) were added to the buffer. The cellular debris was pelleted by centrifugation at 10,000 *g* for 30 min at 4°, and the collected supernatant was mixed with an equal volume of the same extracting buffer but containing in addition 40% (v/v) glycerol. Threonine and tyrosine phosphorylation of p38 MAPK was analyzed according to instructions given in commercially available kits (New England Biolabs, Inc.). The kit employs specific anti-phospho-p38 MAPK antibodies against Thr180/Tyr182 sites that do not cross-react with phosphorylated threonine/tyrosine of extracellular signal-regulated kinase (ERK) 1/2 or c-Jun-NH_2-terminal kinase (JNK). Analysis of Thr180/Tyr182 phosphorylation of p38 MAPK was performed as follows: extracted proteins (20–25 μg) were resolved over sodiumdodecyl sulfate-polyacrylamide gel electrophoresis (SDS-PAGE; 7.5%) gels at RT, blotted onto nitrocellulose membrane, and non-specific binding sites were subsequently blocked. The membrane was probed with specific antibody to phosphorylated threonine and tyrosine of p38 MAPK for primary detection. Anti-rabbit Ig-biotinylated antibody (Amersham Life Science) was employed for secondary detection followed by the addition of streptavidin–HRP conjugate and visualized on film by chemiluminescence. $MAPK^{p38}$ detection using a specific antibody, which recognizes the non-phosphorylated form, was considered as an internal reference for semi-quantitative loading in parallel lanes for each variable. Western blots were scanned by NIH MagiScanII and subsequently quantitated by UN-Scan-IT automated digitizing system (Version 5.1; 32-bit), and the ratio of the density of the band to that of the non-phosphorylated form was performed.

2.5.2. Analysis of Hsp27 phosphorylation by the upstream activated MAPKAP-K2 kinase

Active phosphorylated p38 MAPK regulates a kinase cascade, which may be followed by determining the terminal phosphorylation of Hsp27 by MAPK-activated protein kinase (MAPKAP-K2). After treatment with LPS for the indicated doses and time points, cells were ruptured

in 250 μL of lysis buffer [20 mM HEPES (pH 7.4); 2 mM EGTA; 50 mM β-glycerophosphate; 1 mM Na_3VO_4; 5 mM NaF; 1% (v/v) Triton X-100; 10% (v/v) glycerol; 1 mM DTT; 1 mM PMSF; 10 μg/mL leupeptin; and 10 μg/mL aprotinin] for 30 min on ice. Cell debris was removed by centrifugation at 10,000 *g* for 10 min at 4°. The kinase activity of MAPKAP-K2, which is regulated by the phosphorylation of the upstream p38 MAPK, was assayed with recombinant Hsp27 as a substrate. Briefly, 1 μg of Hsp27 was added to a microcentrifuge tube containing 10 μL (≈10 μg) of cellular extract. Kinase reaction was initiated by the addition of 10 μL of γ-^{32}P-labeled Mg^{2+}/ATP solution (10 mM $MgCl_2$/1 mM ATP/2 μCi of [γ-^{32}P]ATP) and performed at 35° for 20 min. The final concentration of Mg^{2+}/ATP in the assay was adjusted to 2.5 and 0.25 μM, respectively. Reactions were terminated by the addition of 5 μL Laemmli sample buffer and subsequently boiled (95°) for 5 min. Samples were separated by SDS-PAGE [17.5% (w/v) gel]. Gels were blotted onto a Whatmann paper and dried for 2 hr prior to exposure to autoradiography with a phosphorimager, followed by specific quantitation of the corresponding bands.

2.5.3. Assessment of Hsp27 phosphorylation by co-precipitation with MAPKAP-K2 kinase

Epithelial cells were activated with 1 μg/mL LPS (45 min). In some cases, cells were pretreated with 10 μM SB-203580 prior to exposure to LPS. The cells were washed twice in phosphate buffered saline (PBS) and solubilized on ice in lysis buffer (20 mM Tris–HCl, pH 7.4, 150 mM NaCl, 1% Triton X-100, 10% glycerol, 2 mM EDTA, 25 mM glycerophosphate, 20 mM NaF, 1 mM Na_3VO_4, 2 mM sodium pyrophosphate, 1 mM PMSF, 1 μg/mL leupeptin, 5 unit/mL aprotinin) and centrifuged at 15,000 *g* for 20 min at 4°. Endogenous MAPKAP-K2 was precipitated from cell lysates using appropriate antibody for 2 hr at 4°. The G-agarose beads were washed twice with lysis buffer and twice with kinase buffer (25 mM HEPES, pH 7.4, 25 mM $MgCl_2$, 25 mM glycerophosphate, 100 μM sodium orthovanadate, 2 mM dithiothreitol), and the immune complex kinase assays were initiated by the addition of 25 μL of kinase buffer containing 1–5 μg of Hsp27 substrate and 50 μM [γ-^{32}P]ATP (20 Ci/mmol). After 30 min at 30°, the reaction was stopped by the addition of SDS sample buffer and the phosphorylated products analyzed by SDS-PAGE and autoradiography.

2.6. Selective inhibition of p38 MAP kinase and LPS-induced release of pro-inflammatory cytokines

Cells were pre-incubated for 2 hr with SB-203580 (0, 0.01, 0.1, 1, 10, 100 μM) (Calbiochem), a selective inhibitor of p38/RK MAPK. This was followed by exposure to LPS (1 μg/mL) for 24 hr and cell-free supernatants were collected for cytokine analysis (IL-6 and TNF-α) by ELISA [25,26,38], as recounted above.

2.7. Statistical analysis and data presentation

Data are the means and the error bars the SEM. Statistical evaluation of the difference in mean separation was performed by ANOVA, followed by *post hoc* Tukey's test, and the *a priori* level of significance at 95% confidence level was considered at $P \leq 0.05$.

3. Results

3.1. The excitatory role of LPS in mediating the phosphorylation of p38/RK MAPK

The induction of threonine/tyrosine phosphorylation of p38/RK MAPK reflects the activation state of this kinase in regulating the downstream pathway involving MAPKAP-K2. In addition, the role of LPS in mediating the phosphorylation of p38/RK MAPK is not well characterized in the fetal alveolar epithelium. Consequently, we examined the phosphorylation of this kinase in response to LPS in controlled time- and dose-dependent experiments. As shown in Fig. 1A, exposure of alveolar epithelial cells to LPS (1 μg/mL) induced, in a time-dependent manner, the phosphorylation of p38/RK kinase (*p*-p38) on threonine/tyrosine residues. The positive control (+ve control) contained protein extracts prepared from C-6 glioma cells stimulated with anisomycin to induce the phosphorylation of threonine and tyrosine residues of p38/RK kinase. The phosphorylation state-independent p38/RK MAPK is shown in the lower panel of Fig. 1A to verify semi-quantitative loading for gel analysis per loading lane. The amount of p38/RK phosphorylation was quantified by an image analyzer to indicate that the peak of p38/RK phosphorylation due to LPS stimulation is somewhere around the 15-min time point, as shown in the histogram (Fig. 1B). This reference time point (15 min) was subsequently adopted in further experiments. The phosphorylation of p38/RK MAPK became immediately active within minutes post addition of LPS (significantly active at 2 min), continued to increase up until 30 min, thereafter declining, still significantly different at 60 min, but its activity was lost between 90 and 120 min (Fig. 1A and B). Fig. 1C shows the dose-dependent analysis of LPS stimulation (0–1000 ng/mL) at 15 min, indicating a maximum induction of p38/RK phosphorylation at 100–1000 ng/mL concentration range (Fig. 1D). The steady, phosphorylation-independent state (p38) was also quantitated at various doses of LPS (Fig. 1C) to account for equal loading per lane.

3.2. The effect of LPS on the activation of MAPKAP-K2, the downstream kinase controlled by p38/RK MAPK, as assessed by the phosphorylation of its substrate, Hsp27

The activity of MAPKAP-K2 was evaluated by the phosphorylation state of its substrate, Hsp27. A representative

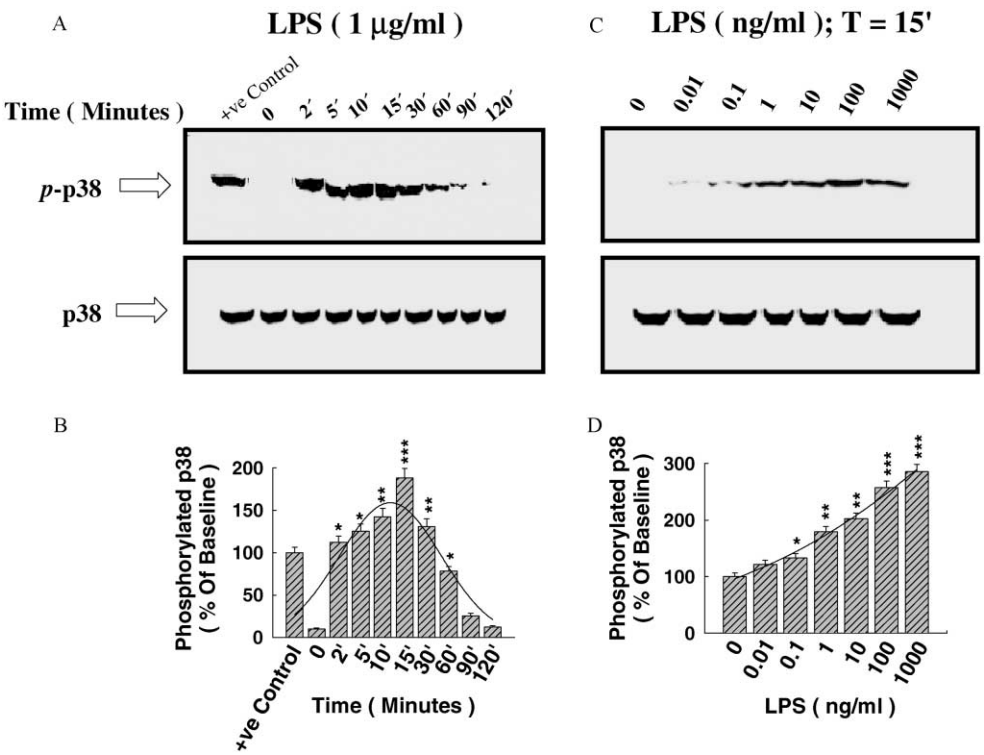

Fig. 1. The immunoregulatory role of LPS in augmenting the phosphorylation and activation of p38 MAPK. Fetal alveolar epithelial cells were stimulated with LPS (1 μg/mL) for the desired time points as indicated. Lysates were separated by a 7.5% SDS-PAGE, transferred to membranes and probed with specific antibodies recognizing p38 and *p*-p38 MAPK. (A) LPS induced, in a time-dependent manner, the phosphorylation of p38, with maximum induction at between 10 and 15 min (*p*-p38 indicates the phosphorylated form and p38 that of the steady-state form). The positive control lane contained loading of extract from anisomycin-treated cells for the recognition of the specificity of phosphorylated p38 bands. (B) Histogram analysis of p38 phosphorylation for the time–response curve and pseudo-Voigt curve fitting showing the peak at 15 min. (C) Dose–response curve showing the effect of LPS (15 min) on p38 phosphorylation, with maximum induction at a concentration of 1000 ng/mL. The lower band indicates non-phosphorylated p38. (D) Histogram analysis of p38 phosphorylation for the dose–response curve and pseudo–Voigt curve fitting showing gradual and maximum induction with LPS; $^{*}P < 0.05$, $^{**}P < 0.01$, $^{***}P < 0.001$, as compared with control (LPS = 0 ng/mL). Here, $n = 3$, which represents the number of independent experiments with separate cell preparations.

Western gel showing the time–response curve of the effect of LPS (1 μg/mL) on Hsp27 phosphorylation (*p*-Hsp27) is shown in Fig. 2A. As shown in Fig. 2A, the peak time for Hsp27 phosphorylation consistently occurred at a later time (30–60 min) than the activation of p38/RK MAPK (15 min). The time peak was determined by histogram analysis of the phosphorylated band, as shown in Fig. 2B. The dose–response curve showing the effect of LPS at 45 min on Hsp27 phosphorylation is shown in Fig. 2C. There was gradual increase in the activity of MAPKAP-K2 as assessed by Hsp27 phosphorylation on LPS exposure, peaking at between 10 and 100 ng/mL, thereafter declining but still statistically significant at 10,000 ng/mL (Fig. 2D).

3.3. The verification of MAPKAP-K2 as a kinase that phosphorylates Hsp27 in vitro

Since Hsp27 is presumed as a downstream substrate of MAPKAP-K2 *in vitro* and *in vivo*, this assumption was verified by co-immunoprecipitation. Inclusion of Hsp27 in the MAPKAP-K2 immune complex kinase reaction resulted in its phosphorylation, as shown in Fig. 3A. Incubation of cell extracts with nothing (control) revealed no Hsp27 phosphorylation in the immune complex (Fig. 3A). Exposure to LPS (1 μg/mL) for 45 min, followed by co-immunoprecipitation, allowed detection of Hsp27 phosphorylation within the complex (Fig. 3A). Pre-treatment with SB-203580 prior to co-immunoprecipitation reduced the phosphorylation of Hsp27. This indicated that Hsp27 is a substrate for MAPKAP-K2 *in vitro*. Fig. 3B displays histogram analysis of Hsp27 phosphorylation.

3.4. The role of p38/RK signaling pathway in mediating the effect of LPS on IL-6 and TNF-α secretion

The activity, but not the activation, of p38/RK MAPK is selectively blocked by the pyridinyl-imidazole compound SB-203580, thereby blockading the downstream pathways associated with the activation of MAPKAP-K2, Hsp27 phosphorylation and pro-inflammatory cytokine transcription and biosynthesis [2]. As shown in Fig. 4A, exposure of alveolar epithelial cells to medium alone for 24 hr had no

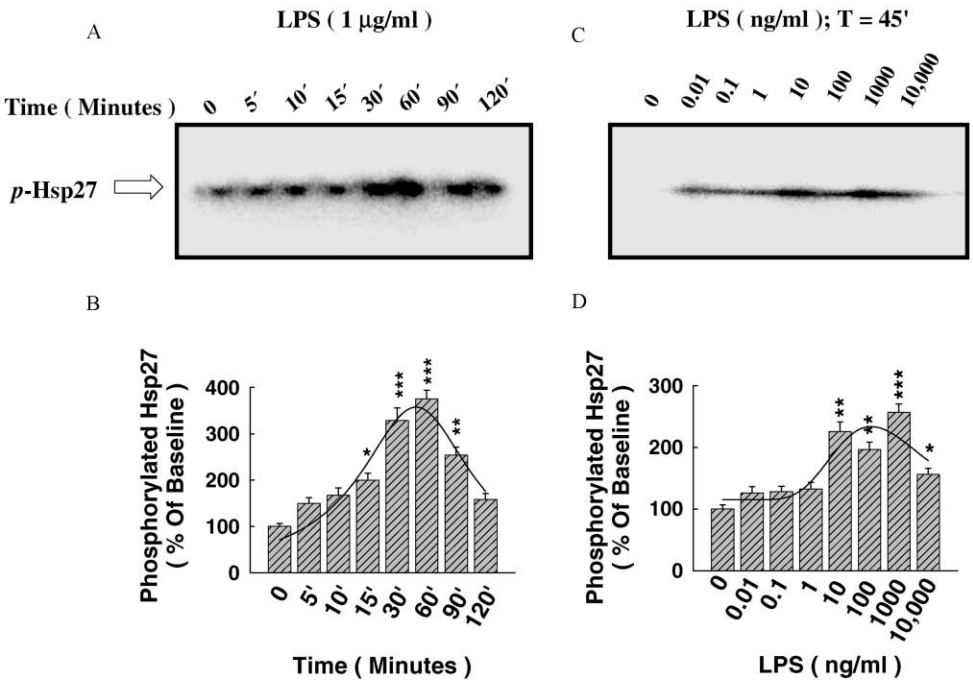

Fig. 2. The regulation by LPS of the activity of MAPKAP-K2, the downstream kinase activated by p38 phosphorylation, through the phosphorylation of its substrate, Hsp27. (A) LPS (1 μg/mL) induced, in a time-dependent manner, the phosphorylation of Hsp27 (*p*-Hsp27), an index of the activity of MAPKAP-K2, with peak analysis at 30–60 min. (B) Histogram analysis of Hsp27 phosphorylation for the time–response curve and pseudo–Voigt curve fitting showing the peak at ≈45 min. (C) Dose–response curve showing the effect of LPS (45 min) on Hsp27 phosphorylation, with maximum induction at a concentration of 1000 ng/mL, thereafter declining. (D) Histogram analysis of Hsp27 phosphorylation for the dose–response curve and pseudo–Voigt curve fitting showing gradual and maximum induction with LPS; $^{*}P < 0.05$, $^{**}P < 0.01$, $^{***}P < 0.001$, as compared with control (LPS = 0 ng/mL). Here, $n = 3$, which represents the number of independent experiments with separate cell preparations.

effect on the release of TNF-α into the supernatant. In addition, pre-treatment with SB-203580 (100 μM) for 2 hr and further exposure to medium alone had no apparent effect on TNF-α secretion. In contrast, administration of LPS (1 μg/mL) for 24 hr enhanced the secretion of TNF-α into the supernatant (Fig. 3A). Pre-treatment with SB-203580, followed by exposure to LPS blockaded, in a dose-dependent manner, LPS-dependent secretion of TNF-α ($IC_{50} = 0.05 \pm 0.01$ μM), as shown in Fig. 3A. Similarly, pre-treatment with SB-203580 blockaded, in a dose-dependent manner, LPS-mediated secretion of IL-6 ($IC_{50} = 3.53 \pm 0.12$ μM) (Fig. 4B). At all concentrations of SB-203580 used, there were no signs of cytotoxicity associated with the treatment, nor there were any decreases in the transepithelial resistance of monolayers (Data not shown).

3.5. The role of N-acetyl-L-cysteine (NAC) in mediating LPS-dependent regulation of pro-inflammatory cytokine production

We have previously shown that NAC, an antioxidant and a precursor of cysteine, the rate-limiting amino acid in the biosynthesis of glutathione (GSH) [10,12–14], suppressed ROS-induced cytokine biosynthesis in a GSH-dependent mechanism [25,26]. Here, NAC suppressed, in a dose-dependent manner, LPS-induced release of TNF-α ($IC_{50} = 26.07 \pm 2.25$ mM) (Fig. 5A) and IL-6 ($IC_{50} = 18.42 \pm 1.75$ mM) (Fig. 5B). Fig. 5A shows the dose-dependent inhibition of LPS-induced TNF-α production due to pre-treatment (2 hr) with NAC. NAC reduced the level of TNF-α approximately 1.3-, 2- and 4-fold relative to LPS alone at 1, 10 and 50 mM, respectively (Fig. 5A). Similarly, NAC reduced, in a dose-dependent manner, the level of IL-6 induced by LPS (Fig. 5B). NAC reduced the level of IL-6 approximately 1.3-, 1.7- and 3.4-fold relative to LPS alone at 1, 10 and 50 mM, respectively (Fig. 5B).

3.6. The role of L-buthionine-(S,R)-sulfoximine (BSO) in mediating LPS-dependent regulation of pro-inflammatory cytokine secretion

We have previously shown that BSO up-regulated intracellular accumulation of ROS and subsequently induced the downstream pathway implicated in cytokine biosynthesis [25,26]. In this study, BSO expectedly augmented, in a dose-dependent manner, LPS-induced release of TNF-α ($EC_{50} = 34.57 \pm 3.87$ μM) (Fig. 6A) and IL-6 ($EC_{50} = 25.21 \pm 3.15$ μM) (Fig. 6B). LPS increased TNF-α secretion by 10-fold above control baseline level and BSO increased the level of TNF-α approximately 1.2 (non-significant), 2- and 1.7-fold relative to LPS alone at 1, 10 and 100 μM, respectively (Fig. 6A). LPS increased IL-6

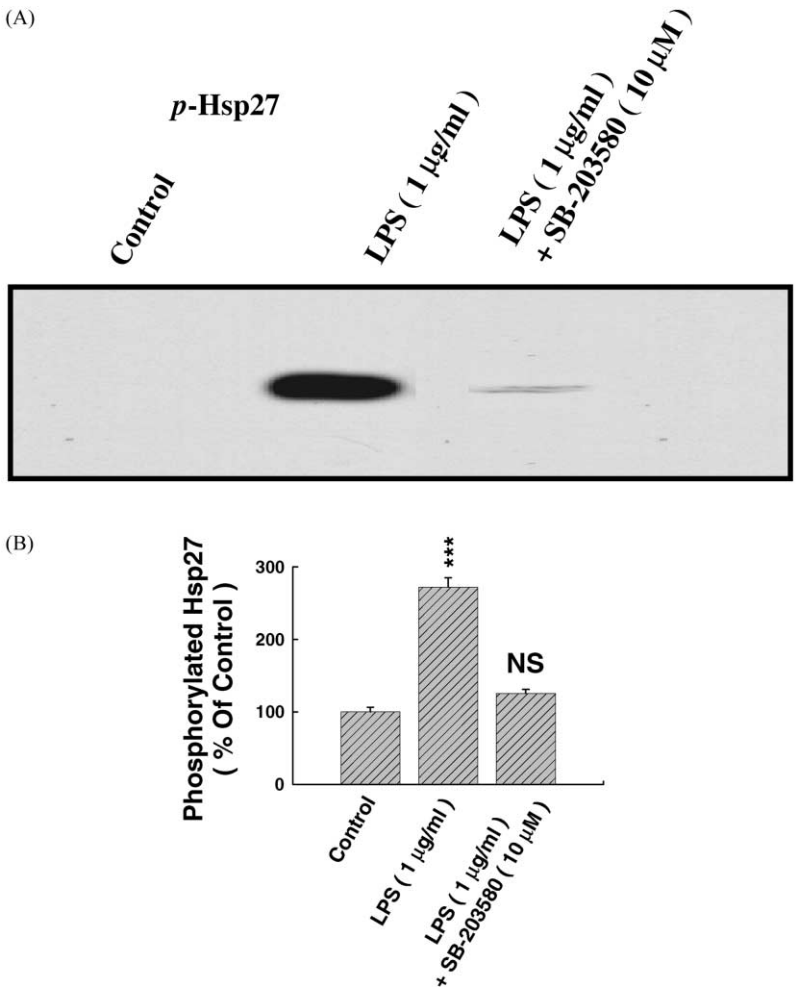

Fig. 3. An immune-complex kinase assay for the co-precipitation of MAPKAP-K2 and the phosphorylation of Hsp27 as a substrate *in vitro*. (A) MAPKAP-K2 was precipitated by a specific antibody in extracts treated with nothing (control), LPS (1 μg/mL) for 45 min or pre-treated with SB-203580 (10 μM) for 2 hr prior to exposure of LPS. The immune-complex containing MAPKAP-K2 mediated the phosphorylation of Hsp27, indicating this protein as a downstream substrate. (B) Histogram analysis of the corresponding bands by phosphorimaging; $^{***}P < 0.001$, as compared with control; NS, non-specific in comparison with control. Here, $n = 3$, which represents the number of independent experiments with separate cell preparations.

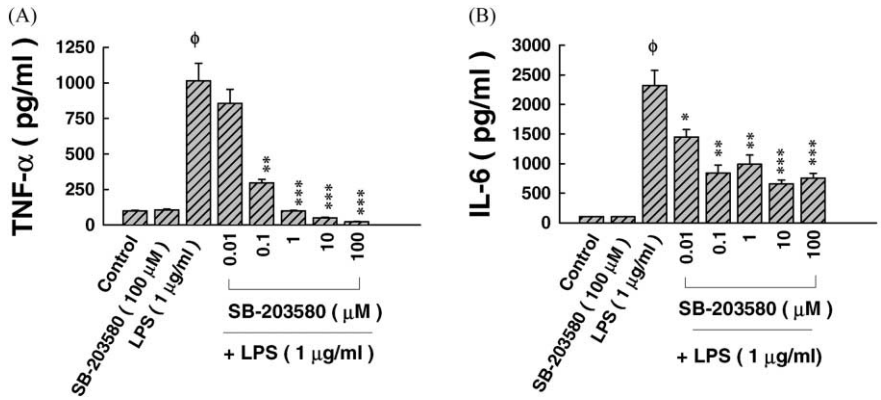

Fig. 4. The effect of selective inhibition of p38 MAPK on LPS-induced TNF-α and IL-6 biosynthesis. (A) Pre-treatment with SB-203580 (2 hr), a selective inhibitor of p38 MAPK, prior to exposure to LPS (1 μg/mL), reduced LPS-induced TNF-α production in a dose-dependent manner. LPS up-regulated the secretion of TNF-α approximately 4-fold relative to cells incubated in medium alone (control). Pre-treatment with SB-203580 (100 μM) on its own did not affect TNF-α synthesis. SB-203580 reduced LPS-induced TNF-α secretion at doses $\geq$0.1 μM, with maximum inhibition at 100 μM. (B) Pre-treatment with SB-203580 (2 hr), prior to exposure to LPS (1 μg/mL), reduced LPS-induced IL-6 production in a dose-dependent manner. LPS up-regulated the secretion of IL-6 approximately 24-fold relative to cells incubated in medium alone (control). Pre-treatment with SB-203580 (100 μM) on its own did not affect IL-6 synthesis. SB-203580 reduced LPS-induced IL-6 secretion at doses $\geq$0.01 μM, with maximum inhibition at 100 μM. Here, $n = 4$, which represents the number of independent experiments with separate cell preparations.

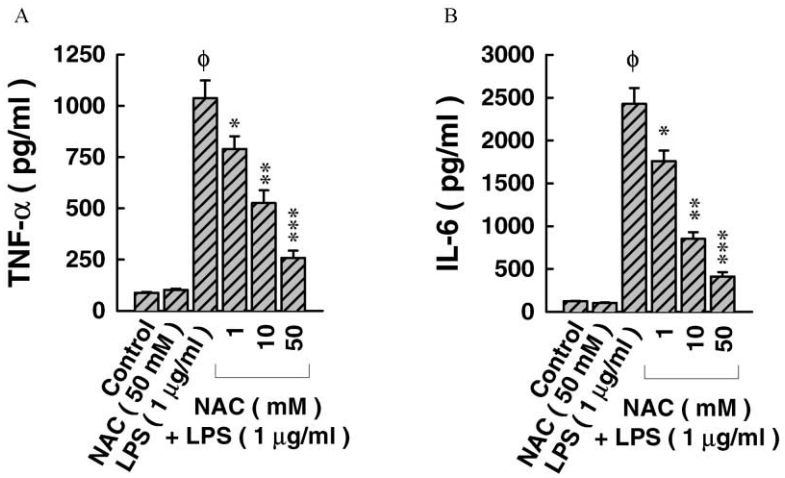

Fig. 5. The effect of NAC on LPS-mediated pro-inflammatory cytokine biosynthesis. (A) Pre-treatment with NAC (2 hr) before stimulating with LPS (1 μg/mL) reduced, in a dose-dependent manner, the induction of TNF-α, effective at doses ≥1 mM, with maximum suppression at 50 mM. Pre-treatment with NAC (50 mM) on its own had no apparent effect on the secretion of TNF-α. (B) Pre-treatment with NAC (2 hr) before stimulating with LPS (1 μg/mL) reduced, in a dose-dependent manner, the induction of IL-6, effective at doses ≥1 mM, with maximum suppression at 50 mM. Pre-treatment with NAC (50 mM) on its own had no apparent effect on the secretion of IL-6; $^{\phi}P < 0.05$, as compared with control; $^{*}P < 0.05$, $^{**}P < 0.01$, $^{***}P < 0.001$, as compared with LPS (1 μg/mL). Here, $n = 4$, which represents the number of independent experiments run in duplicate with separate cell preparations.

secretion by 21-fold above control baseline level and BSO increased the level of IL-6 approximately 1.7-, 3.6- and 3.7-fold relative to LPS alone at 1, 10 and 100 μM, respectively (Fig. 6B).

3.7. The role of NAC in mediating glutathione (GSH) biosynthesis

The cysteine that is provided due to NAC administration is eventually fed into the biosynthetic pathway that brings about the formation of GSH by the action of γ-glutamylcysteine synthetase (γ-GCS), the rate-limiting enzyme in the biosynthesis of GSH [10,11,13]. Incubation of alveolar epithelial cells for 24 hr with NAC induced, in a dose-dependent manner, the intracellular accumulation of GSH (Fig. 7A). This effect was associated with a dose-dependent decrease in the intracellular level of the GSSG, as reflected by an increasing redox ratio of GSH/GSSG (Fig. 7A). The time–response curve for NAC incubation at 50 mM is shown in Fig. 7B. Incubating cells with NAC for different time points induced the intracellular formation of GSH and reduced the levels of GSSG (Fig. 7B). Within 2 hr of NAC incubation, there was significant accumulation of GSH, the concentration of which continued to elevate in the continuing presence of NAC and maximized at around 16–24 hr, thereafter declining (48 hr) but persistently found

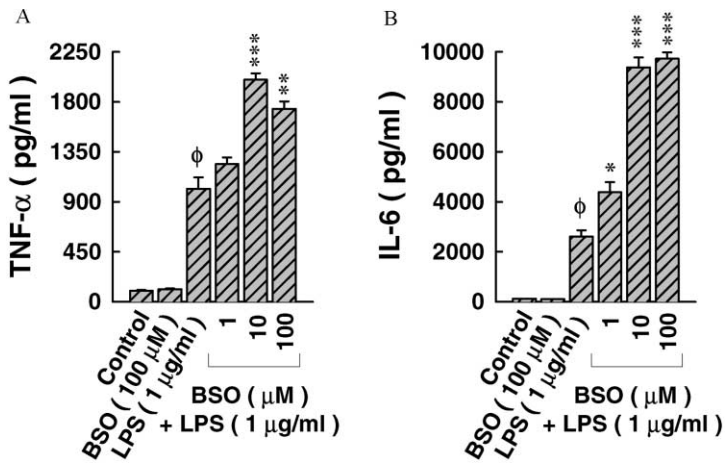

Fig. 6. The effect of BSO on LPS-mediated pro-inflammatory cytokine biosynthesis. (A) Pre-treatment with BSO (2 hr) before stimulating with LPS (1 μg/mL) augmented, in a dose-dependent manner, the induction of TNF-α, effective at doses ≥10 μM, with maximum amplification at 100 μM. Pre-treatment with BSO (100 μM) on its own had no apparent effect on the secretion of TNF-α. (B) Pre-treatment with BSO (2 hr) before stimulating with LPS (1 μg/mL) reduced, in a dose-dependent manner, the induction of IL-6, effective at doses ≥1 μM, with maximum induction at 100 μM. Pre-treatment with BSO (100 μM) on its own had no apparent effect on the secretion of IL-6; $^{\phi}P < 0.05$, as compared with control; $^{*}P < 0.05$, $^{**}P < 0.01$, $^{***}P < 0.001$, as compared with LPS (1 μg/mL). Here, $n = 4$, which represents the number of independent experiments run in duplicate with separate cell preparations.

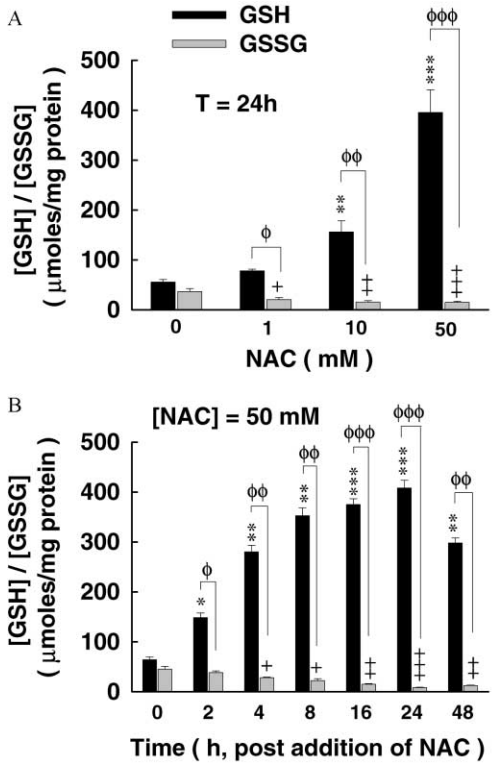

Fig. 7. The effect of NAC on intracellular redox potential (GSH/GSSG). (A) Cells were exposed to NAC treatment for 24 hr, thereby inducing the intracellular accumulation of the reduced form of glutathione (GSH) in a dose-dependent manner. Intracellular accumulation of GSH due to NAC was at the expense of the oxidized form of glutathione (GSSG), as evident from the reduced GSSG/GSH ratio. (B) Time-dependent analysis of the effect of NAC (50 mM) on GSH and GSSG accumulation. GSH concentration prevailed with NAC treatment, statistically significant as early as 2 hr post-incubation with NAC, thereafter ascending to a maxima at 24 hr, declining, but still persistently significant, at 48 hr. This elevation of intracellular GSH due to NAC is partly at the expense of GSSG, as shown from the reduced GSSG/GSH equilibrium ratio; $^{\phi}P < 0.05$, $^{\phi\phi}P < 0.01$, $^{\phi\phi\phi}P < 0.001$, for [GSH] as compared with [GSSG]; $^{*}P < 0.05$, $^{**}P < 0.01$, $^{***}P < 0.001$, as compared with control (NAC at 24 hr and NAC at 50 mM); $^{+}P < 0.05$, $^{++}P < 0.01$, $^{+++}P < 0.001$, for [GSSG] as compared with $[GSSG]_{control}$.

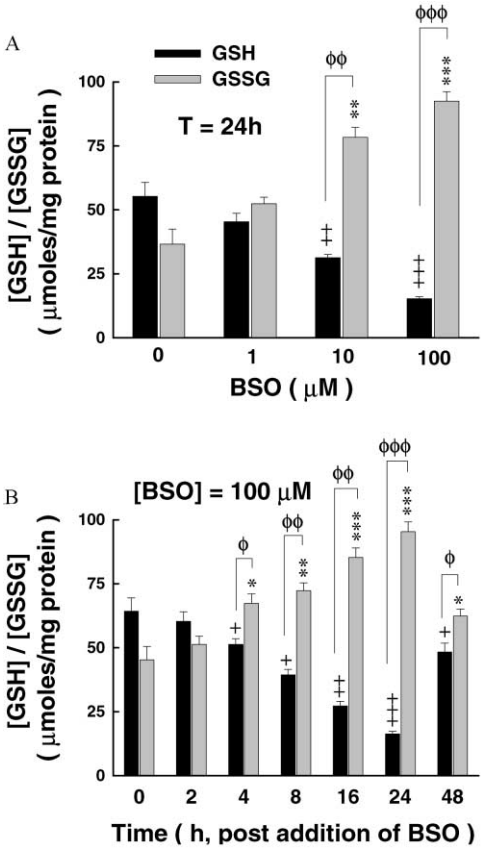

Fig. 8. The effect of BSO on intracellular redox potential (GSH/GSSG). (A) Cells were exposed to BSO treatment for 24 hr, thereby inducing the intracellular accumulation of the oxidized form of glutathione (GSSG) in a dose-dependent manner. Intracellular accumulation of GSSG due to BSO was at the expense of the reduced form of glutathione (GSH), as evident from the reduced GSH/GSSG ratio. (B) Time-dependent analysis of the effect of BSO (100 μM) on GSH and GSSG accumulation. GSSG concentration prevailed with BSO treatment, statistically significant at 4 hr post-incubation with BSO, thereafter ascending to a maxima at 24 hr, declining, but still persistently significant, at 48 hr. This elevation of intracellular GSSG due to BSO is partly at the expense of GSH, as shown from the reduced GSH/GSSG equilibrium ratio; $^{\phi}P < 0.05$, $^{\phi\phi}P < 0.01$, $^{\phi\phi\phi}P < 0.001$, for [GSH] as compared with [GSSG]; $^{*}P < 0.05$, $^{**}P < 0.01$, $^{***}P < 0.001$, as compared with control (BSO at 24 hr and BSO at 100 μM); $^{+}P < 0.05$, $^{++}P < 0.01$, $^{+++}P < 0.001$, for [GSH] as compared with $[GSH]_{control}$.

to be still significantly different from control deproteinated monolayers (Fig. 7B).

3.8. The role of BSO in mediating glutathione (GSSG) biosynthesis

During the reduction of ROS by glutathione, GSH is converted into GSSG by the glutathione–peroxidase coupled reaction [13]. The formed GSSG is rapidly recycled back to GSH by the action of glutathione reductase or extruded into the interstitial fluid bathing the alveoli [13,14]. Incubation of epithelial cells for 24 hr with BSO induced, in a dose-dependent manner, the intracellular accumulation of GSSG (Fig. 8A). This effect was associated with a dose-dependent decrease in the intracellular level of the GSH, as reflected by an increasing redox ratio of GSSG/GSH (Fig. 8A). The time–response curve for BSO incubation at 100 μM is shown in Fig. 8B. Incubating cells with BSO for different time points induced the intracellular formation of GSSG and reduced the levels of GSH (Fig. 8B). Within 4 hr of BSO incubation, there was significant accumulation of GSSG, the concentration of which continued to elevate in the continuing presence of BSO and maximized at around 16–24 hr, thereafter declining (48 hr) but persistently found to be still significantly different from control deproteinated monolayers (Fig. 8B).

3.9. The role of NAC in regulating the p38/RK MAPK signaling pathway

The amount of threonine/tyrosine phosphorylation of p38/RK MAPK was reduced, in a dose-dependent manner,

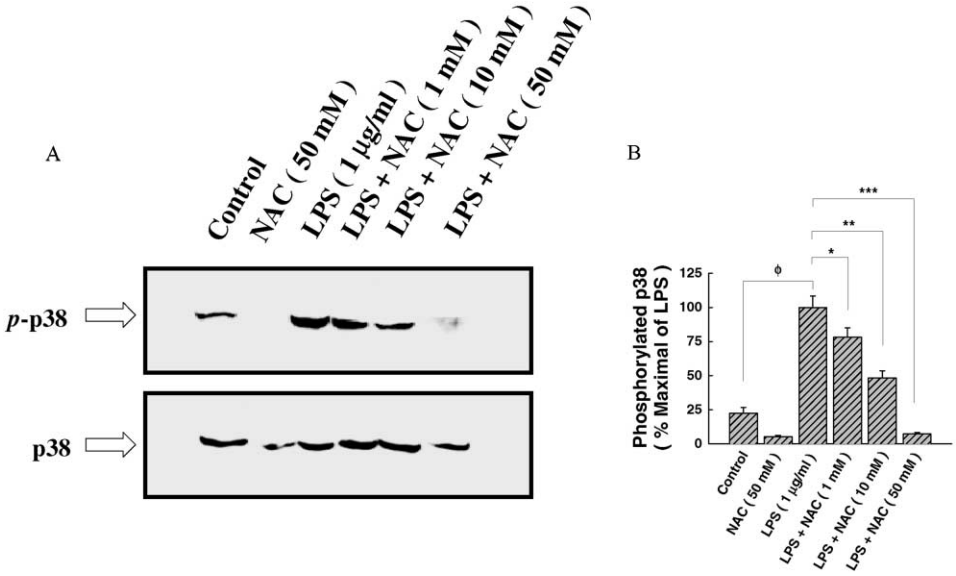

Fig. 9. The attenuating effect of NAC on p38/RK phosphorylation. (A) Epithelial cells were cultured with medium alone (control), pre-treated with NAC (50 mM) for 2 hr prior to exposure to medium alone for 15 min, exposed to LPS (1 μg/mL) for 15 min or pre-treated with NAC (1–50 mM) for 2 hr followed by exposure to LPS (1 μg/mL) for 15 min. Lysates were separated by a 7.5% SDS-PAGE and probed with specific antibodies directed against the phosphorylated threonine/tyrosine residues of p38/RK MAPK or the phosphorylation-independent state of p38. Pre-treatment with NAC (50 mM) followed by exposure to medium alone did not affect the phosphorylation of p38/RK, despite the observation it abolished the faint band appearing under the control lane. Pre-treatment with NAC attenuated the phosphorylation-mediated effect of LPS, in a dose-dependent manner, completely blocking its phosphorylation at 50 mM. The steady state of p38 is largely not affected with any of the aforementioned treatments. (B) Histogram analysis of p38 phosphorylation for the inhibitory dose–response curve of NAC; $^{\phi}P < 0.05$, as compared with control; $^{*}P < 0.05$, $^{**}P < 0.01$, $^{***}P < 0.001$, as compared with control (LPS = 1 μg/mL). Here, $n = 3$, which represents the number of independent experiments with separate cell preparations.

with NAC pre-treatment (2 hr) prior to exposure to LPS (1 μg/mL) for 15 min (Fig. 9A). LPS-mediated phosphorylation of p38/RK MAPK was maximally blockaded with NAC at 50 mM. The steady, phosphorylation-independent state of p38/RK is shown in the lower panel of Fig. 9A. The dose–response curve exhibiting the inhibitory effect of NAC on p38/RK phosphorylation state is given in a form of histogram analysis in Fig. 9B.

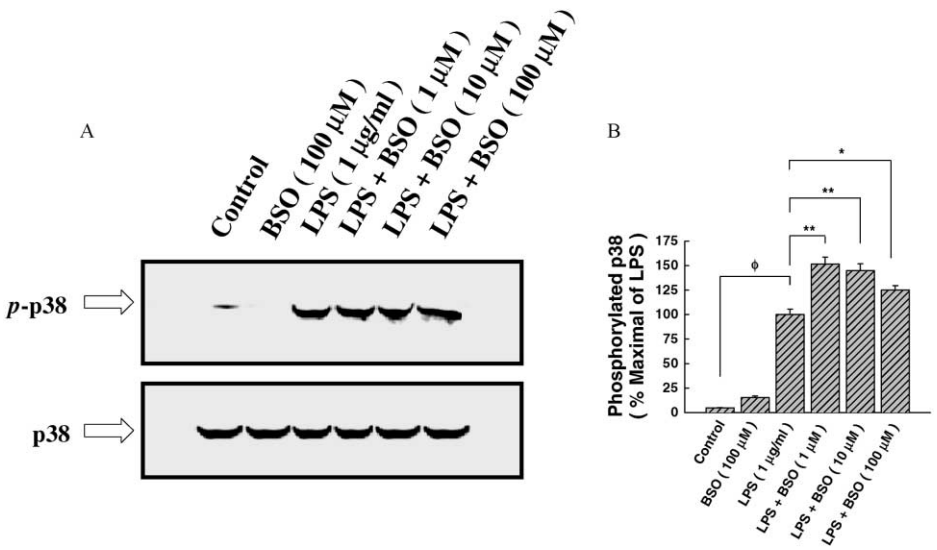

Fig. 10. The excitatory effect of BSO on p38/RK phosphorylation. (A) Epithelial cells were cultured with medium alone (control), pre-treated with BSO (100 μM) for 2 hr prior to exposure to medium alone for 15 min, exposed to LPS (1 μg/mL) for 15 min or pre-treated with BSO (1–100 μM) for 2 hr followed by exposure to LPS (1 μg/mL) for 15 min. Lysates were separated by a 7.5% SDS-PAGE and probed with specific antibodies directed against the phosphorylated threonine/tyrosine residues of p38/RK MAPK or the phosphorylation-independent state of p38. Pre-treatment with BSO (100 μM) followed by exposure to medium alone did not affect the phosphorylation of p38/RK. Pre-treatment with BSO augmented the phosphorylation-mediated effect of LPS, in a dose-dependent manner. The steady state of p38 is largely not affected with any of the aforementioned treatments. (B) Histogram analysis of p38 phosphorylation for the inhibitory dose–response curve of BSO; $^{\phi}P < 0.05$, as compared with control; $^{*}P < 0.05$, $^{**}P < 0.01$, $^{***}P < 0.001$, as compared with control (LPS = 1 μg/mL). Here, $n = 3$, which represents the number of independent experiments with separate cell preparations.

3.10. The role of BSO in regulating the p38/RK MAPK signaling pathway

The amount of threonine/tyrosine phosphorylation of p38/RK MAPK was augmented, in a dose-dependent manner, with BSO pre-treatment (2 hr) prior to exposure to LPS (1 μg/mL) for 15 min (Fig. 10A). LPS-mediated phosphorylation of p38/RK MAPK was maximally amplified with BSO at 1–10 μM. The steady, phosphorylation-independent state of p38/RK is shown in the lower panel of Fig. 10A. The dose–response curve exhibiting the excitatory effect of BSO on p38/RK phosphorylation state is given in a form of histogram analysis in Fig. 10B.

4. Discussion

There is increasing evidence implicating the alveolar epithelium, in particular, as a dynamic barrier that plays an important role in regulating the inflammatory and metabolic responses to oxidative stress and the accompanying inflammatory signal, sepsis, endotoxemia, and other critical illnesses in the lung [17,25,26,38,40,41]. The respiratory epithelium is a primary target of an inflammatory/infectious condition at the epithelial–blood interface and is itself capable of amplifying an inflammatory signal by recruiting inflammatory cells and by producing inflammatory mediators. Many of the side effects of LPS, derived form the cell wall of Gram negative bacteria, are secondary to the overproduction of pro-inflammatory mediators [42]. Inflammatory as well as autoimmune disease is often associated with deregulated expression and biosynthesis of pro-inflammatory cytokines, including TNF-α and IL-6, which influence a plethora of cellular functions. Therefore, the down-regulation of an inflammatory signal is a major focus of the rational approach to the treatment of inflammatory diseases, such as chronic inflammation, sepsis and rheumatoid arthritis. For instance, a novel recent study by Haskó *et al.* [43] reported a potential role for extracellular purines, including adenosine and ATP, and inosine, a degradation product of these purines, as potent endogenous immunomodulatory molecules that inhibit inflammatory cytokine biosynthesis and protect against endotoxin-induced shock. It has also been reported, in addition, that selective inhibition of phosphodiesterases, a family of enzymes involved in the degradation of cAMP/cGMP [44,45], steroids, such as glucocorticoids [46], pyrimidyl-piperazine derivatives [47–50], and ERK and p38/RK MAPK selective inhibitors [2,3] differentially regulate the transcription and biosynthesis of inflammatory cytokines.

The novel mammalian p38 MAPK was originally identified in murine pre-B lymphocytes transfected with the LPS-complex receptor CD14 and in murine macrophages where it was activated in response to LPS [51]. In parallel, p38 MAPK was also identified as a reactivating kinase (RK), which activates MAPKAP-K2 (MK-2), which in turn phosphorylates the small heat-shock protein, Hsp27, and regulates the stability of cytokine transcripts bearing the pentanucleotide sequence of AU-rich elements (AREs) [2,3,9,52]. Of note, p38 MAPK and the downstream pathway regulated are essentially crucial for LPS-induced cytokine gene expression and biosynthesis [2,3,5,53,54]. For instance, knockout mice lacking MK-2 (MK-$2^{-/-}$) exhibited a colossal reduction in the biosynthesis of TNF-α, a potent pro-inflammatory cytokine that is involved in many human diseases [1,40,55,56], and are remarkably resistant to shock induced by LPS [57]. Recent evidence, furthermore, suggested that the p38/RK MAPK/MK-2 pathway is redox-sensitive and governs the transcription and biosynthesis of pro-inflammatory cytokines in a redox-dependent mechanism [40,58–60]. However, redox regulation of the p38/RK MAPK/MK-2 pathway mediating cytokine signaling in the fetal alveolar epithelium is not well characterized. It was subsequently hypothesized that p38/RK MAPK-mediated regulation of LPS-dependent TNF-α/IL-6 biosynthesis is redox-sensitive, and that intracellular glutathione manipulation modulates the capacity of the epithelium to produce these inflammatory cytokines.

The signal transduction cascade that regulates the biosynthesis and secretion of inflammatory cytokines in the fetal alveolar epithelium has not been well defined. Administration of LPS, derived from *E. coli*, up-regulated the extracellular accumulation of TNF-α/IL-6 and other cytokines [25,26,38]. The effects of LPS are essentially mediated by the membrane-bound CD14 complex and, in part, through the circulating lipopolysaccharide-binding protein (LBP) [42,61]. It was reported, furthermore, that LPS-mediated responses on cytokine transcription and biosynthesis bifurcate at the level of Ras/Raf G-coupled proteins into two major signaling pathways: One that runs through the nuclear factor-κB (NF-κB) inducing kinase (NIK) route, which regulates the phosphorylation of the inhibitory-κB (IκB) proteins, the cytosolic inhibitors of NF-κB, and another which is mediated through the ERK and p38/RK MAPK pathways [2,3,62] (Fig. 11). The transmission of the signaling cascade across the membrane is associated with the activation of upstream kinases that diverge at either activating the p38 mitogen-activated protein kinase pathway or the IκB/NF-κB pathway. Small G-coupled protein, such as PAK and RAC, mediate the activation of mitogen-activated protein kinase kinase kinase (MEKK) or NF-κB inducing kinase (NIK), at which level the converging pathways bifurcates into two branches. One pathway activates IκB kinase (IKK), thereby leading to IκB phosphorylation/degradation and subsequently allowing NF-κB complex to translocate to the nucleus and promote gene expression. Another pathway involves the phosphorylation of MAPK kinase (MKK), which phosphorylates and activates $MAPK^{p38}$. This pathway is selectively blocked by the pyridinyl-imidazole,

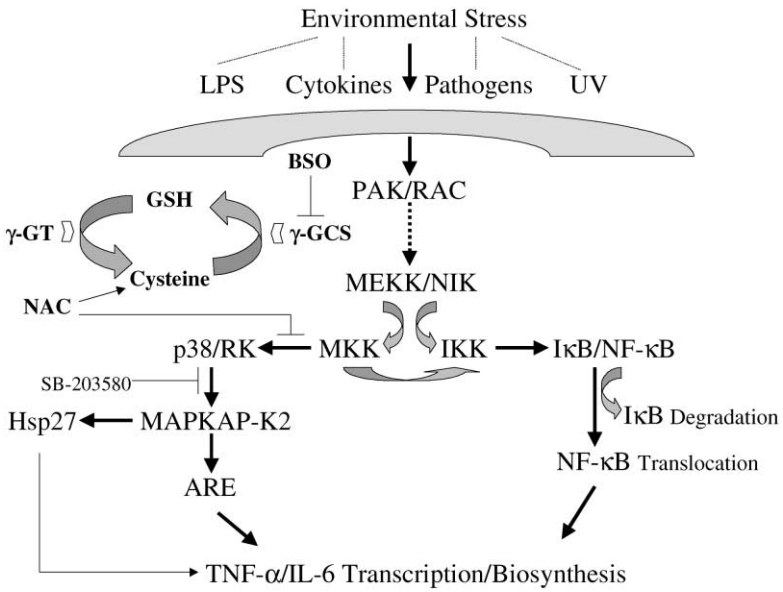

Fig. 11. Schematic showing environmental stresses, such as LPS, cytokines, pathogens and irradiation (UV), in mediating redox signal transduction pathways regulating cytokines in the alveolar epithelium (for details see Section 4).

SB-203580. The activation of the $MAPK^{p38}$ pathway regulates the downstream activation of MAPKAP, which phosphorylates the small Hsp27 and activates the stability of transcripts of cytokines bearing the ARE. Whether Hsp27 directly regulates TNF-α/IL-6 transcription and biosynthesis has yet to be ascertained, although recent evidence suggested that it posses cyto-regulatory potential. The antioxidant NAC provides cysteine that feeds into the biosynthetic machinery allowing the formation of GSH by the action of the rate-limiting enzyme, γ-GCS, which is blocked by the action of BSO. GSH is broken down to cysteine by the action of γ-glutamyl transpeptidase, a membrane-bound enzyme. Redox regulation of the $MAPK^{p38}$ pathway mediated by NAC is likely to implicate the blockading of the upstream kinase that leads to phosphorylation and activation of p38/RK.

Exposure to LPS induced, in a time- and dose-dependent manner, the phosphorylation of p38/RK MAPK, suggesting the involvement of an upstream kinase, such as MKK, in LPS-mediated regulation of the $MAPK^{p38}$ pathway [63]. Similar to other MAPK families, $MAPK^{p38}$ is activated by dual phosphorylation of Thr and Tyr in the so-called Thr-Gly-Tyr activation loop or motif [2,3,63]. Upon stimulation, $MAPK^{p38}$ phosphorylates and activates the MK-2 pathway, which regulates the phosphorylation of Hsp27. The biological activity of $MAPK^{p38}$ is selectively blocked by the pyridinyl-imidazole compound SB-203580, which is postulated to possess anti-inflammatory activity [63]. In this respect, SB-203580 has been reportedly associated with the suppression and/or augmentation of the transcription and biosynthesis of a wide array of inflammatory and anti-inflammatory mediators, including IL-1β [53], IL-6, IL-8 [30,64], IL-10 [65,66], IL-12 [63], TNF-α [9,67,68] and prostaglandin-E_2 (PGE_2) [69]. The results therein reported jibe with the proposal that selective blockading of the $MAPK^{p38}$ signaling transduction pathway exerts an anti-inflammatory condition via suppression of the release of inflammatory mediators, including TNF-α and IL-6. Although from the present data alone, we could not infer whether the Hsp27 pathway, which is an immediate pathway regulated by the upstream kinase MK-2, is likely to exert a direct immunoregulatory effect on cytokine biosynthesis, it is possible that Hsp27 might be implicated. This assumption is rather reinforced by recent evidence suggesting that Hsp27 can act as an endogenous protein circulating in the serum of breast cancer patients and a protein whose induction correlates with the onset of LPS shock [66]. Moreover, it has been reported that Hsp27 mediates regulatory effects on the biosynthesis of TNF-α through an IL-10-dependent mechanism, a pathway known to exert an anti-inflammatory role in several systems [63,66].

Redox signaling regulating $MAPK^{p38}$-mediated induction of pro-inflammatory cytokines, and particularly TNF-α/IL-6, has not been well characterized. It has been recently reported that ROS-initiated and redox-sensitive mechanisms converge on $MAPK^{p38}$-mediated regulation of cytokine signaling in a cascade circuit, emphasizing the highly organized interactive nature of intracellular signals emanating from cell membranes leading to gene regulation and induction [58]. Furthermore, a novel glutathione-ensitive antioxidant response element regulating the $MAPK^{p38}$ cascade was reported in mediating the inducible expression of phase II enzymes, such as rGSTA2, known to be responsible for the protective adaptive responses to electrophiles and ROS [59]. In a much recent investigation, Hashimoto *et al.* [30] reported a dual role for NAC in attenuating TNF-α-induced p38 MAPK activation and p38 MAPK-mediated IL-8 biosynthesis *in vitro*. In the present

study, LPS-mediated secretion of TNF-α was attenuated by selectively blockading the p38/RK MAPK/MK-2 pathway and that p38/RK MAPK-mediated regulation of TNF-α/IL-6 biosynthesis was shown to be redox-sensitive and modulated by the antioxidant and glutathione (GSH) precursor, NAC. NAC, a cysteine pro-drug [14,28,70], can suppress cytokine production [19,20,22,26] and protect against ROS-mediated lung injury [28]. The rate-limiting substrate for GSH biosynthesis is glutamate–cysteine ($K_{\text{m glutamate}} = 1.6-2$ mM; $K_{\text{m cysteine}} = 0.3$ mM) [10,26,28,70]. Replenishing and sustaining intracellular GSH concentrations, therefore, is accomplished by administering compounds that increase the level of this amino acid (cysteine) or by promoting the activity of γ-GCS, the rate-limiting enzyme in the biosynthesis of GSH [10,31]. The ability of NAC to induce intracellular accumulation of GSH suggested that its potential to suppress cytokine secretion resides on two possible pathways: firstly, the amino acid cysteine provided by the administration of NAC eventually feeds into the biosynthetic machinery regulated by γ-GCS. GSH that is formed during this conversion reduces ROS through the glutathione–peroxidase coupled reaction [13]. Therefore, the pathway implicated with cysteine is to complement the biosynthetic process, where GSH can directly scavenge ROS. Secondly, NAC has antioxidant properties in that it is capable of directly scavenging and dissimulating accumulating ROS [70]. We have previously shown that NAC induced intracellular formation of GSH [13,14], consistent with the observation reported in this study, and that NAC ability to detoxify intracellular ROS blockaded the regulated downstream pathway for cytokine signaling [25,26]. Taken together, these data argue for ROS as potential messengers in regulating cytokine signaling and that the ability of NAC to blockade this pathway resides in its potential either to deliver GSH, a major antioxidant thiol or to reduce excess ROS accumulation [13,28,70].

The GSH biosynthetic pathway is selectively blocked by BSO, a specific and irreversible inhibitor of γ-GCS [10,14,31]. Consequently, the capacity of the epithelium to replenish intracellular stores of GSH is dramatically affected, thereby modulating the optimum equilibrium necessary to evoke a defense strategy in pathophysiology [13,14]. Redox disequilibrium imposed by BSO as evident from reversing the GSH/GSSG ratio subsequently leads to ROS up-regulation, whose inappropriate disposition, accumulation and intracellular localization augment a pro-inflammatory signal that is dependent, in part, on the activation of redox-sensitive transcription factors [15,62]. I believe that the pathway mediating BSO-induced up-regulation of cytokines in the alveolar epithelium involves a mediator, the most likely candidate being the hydroxyl radical ($^{\bullet}$OH) [25]. This conforms to the evidence that GSH is involved in H_2O_2 reduction, a major source of $^{\bullet}$OH, through the glutathione–peroxidase coupled reaction [11,13], suggesting that in the case of BSO pre-incubation, GSH depletion seems involved in its effect [25,26]. It is possible that GSH depletion by blocking its biosynthesis reduces the capacity of the epithelium to dispose accumulating H_2O_2, with the resulting increase in $^{\bullet}$OH production. It remains to be defined, however, whether GSH depletion is implicated in up-regulating cytokines in association with lung disease, since the degree of depletion necessary to evoke cytokines *in vitro* is higher than that observed in pathophysiology *in vivo* [12,15,20,25,26].

The novel antioxidant potential of NAC was also associated with the ability to suppress the phosphorylation and activation of the $MAPK^{p38}$ pathway, in contrast to the effect of BSO, which augmented this pathway, ostensibly due to ROS accumulation. Since ROS, derived from exposure to extracellular signals inducing stress, were reported to activate the $MAPK^{p38}$ pathway [2,3,63], the possibility of NAC effectively acting as an antioxidant blockading this cascade is very probable. However, the possibility that NAC might be directly interacting with the one or more of the components of the $MAPK^{p38}$ module and whether it is blockading upstream kinases converging onto this pathway cannot be excluded. On the mechanism of action of NAC, as a thiol-modulating agent, in blockading the $MAPK^{p38}$ pathway, we report the likely occurrence of several possible mechanisms. ROS, such as $O_2^{\bullet -}$, H_2O_2 and $^{\bullet}$OH may function as second messengers in signal transduction. Although MAPKs may be directly activated by oxidants, the role of ROS in the activation of the MAPKs pathway by cytokines is largely inferred on the basis of the inhibition of MAPKs by NAC [60]. It was also been reported that NAC acts as an inhibitor of the JNK pathway regulated by TNF-α [71] and that TNF-α stimulation of $MAPK^{p42/44}$, $MAPK^{p38}$ and $MAPK^{JNK}$ pathways was blockaded by NAC under serum-free conditions [60]. Furthermore, apoptosis signal-regulating kinase-1 (ASK-1) was recently identified as a MAP kinase kinase that activates the $MAPK^{p38}$ pathway [72]. Additionally, it was shown that TNF-α-mediated regulation of ASK-1 is ROS- and redox-sensitive and that NAC and TRX, a redox molecule, blockaded the dimerization and the activity of ASK-1 [30,72]. Subsequently, it was hypothesized that ASK-mediated regulation of the MAPK cascades depends on the interaction of ASK with the reduced form of a thiol modulating agent (NAC, GSH, TRX), thereby causing direct inhibition of the activity of the downstream pathway [72]. Although the activity of ASK-1 has not been assessed in this investigation, it is very likely that $MAPK^{p38}$-mediated regulation of TNF-α/IL-6 biosynthesis involves a ROS/redox-sensitive mechanism regulating the activity of ASK-1 and probably other components of the converging upstream cascades, thereby attenuating the stimulatory effect of p38/RK pathway in cytokine signaling. Collectively, the $MAPK^{p38}$ pathway seems to be directly involved in cytokine signaling and that $MAPK^{p38}$-mediated regulation of LPS-induced TNF-α/IL-6 biosynthesis is ROS/redox-sensitive.

In summary, the results of the present investigation could be highlighted as follows: (i) exposure to *E. coli*-derived LPS induced a time- and dose-dependent activation of the $MAPK^{p38}$ pathway; (ii) LPS-mediated regulation of $MAPK^{p38}$ cascade was associated with the activation of the MK-2 pathway, thereby allowing phosphorylation of Hsp27; (iii) selective blockading of the $MAPK^{p38}$ pathway attenuated TNF-α/IL-6 biosynthesis induced by LPS; (iv) NAC reduced LPS-induced TNF-α/IL-6 secretion, an effect associated with its ability to induce intracellular accumulation of GSH and lower that of GSSG; (v) the antioxidant potential of NAC and its ability to feed cysteine onto the GSH biosynthetic machinery are likely to reside in its effectiveness to blockade the $MAPK^{p38}$ pathway, thereby suppressing the downstream cytokine signaling pathway; (vi) BSO augmented LPS-mediated cytokine biosynthesis, an effect associated with the ability to induce intracellular accumulation of GSSG and lower that of GSH; and (vii) the ability of BSO to induce intracellular accumulation of ROS due to redox disequilibrium imposed is likely to reside in its effectiveness to augment the $MAPK^{p38}$ pathway and the downstream cytokine signaling mechanism. It is concluded that $MAPK^{p38}$-mediated regulation of LPS-induced cytokine production in the alveolar epithelium requires the involvement of redox-mediated signaling pathways.

Acknowledgments

This work was supported by grants from the Medical Research Council (MRC, UK), Anonymous Trust and Tenovus-Scotland. John Haddad is a recipient of the George John Livanos prize (London).

References

[1] Herlaar E, Brown Z. p38 MAPK signalling cascades in inflammatory disease. Mol Med Today 1999;5:439–47.
[2] Garrington TP, Johnson GL. Organization and regulation of mitogen-activated protein kinase signalling pathways. Curr Opin Cell Biol 1999;11:211–8.
[3] Su B, Karin M. Mitogen-activated protein kinase cascades and regulation of gene expression. Curr Biol 1996;8:402–11.
[4] Stein B, Yang MX, Young DB, Janknecht R, Hunter T, Murray BW, Barbosa MS. p38-2, a novel mitogen-activated protein kinase with distinct properties. J Biol Chem 1997;272:19509–17.
[5] Lee JC, Laydon JT, Mcdonnell PC, Gallagher TF, Kumar S, Green D, Mcnulty D, Blumenthal MJ, Heys JR, Landvatter SW, Strickler JE, Mclaughlin MM, Siemens IR, Fisher SM, Livi GP, White JR, Adams JL, Young PR. A protein kinase involved in the regulation of inflammatory cytokine biosynthesis. Nature 1994;372:739–46.
[6] Wang XS, Diener K, Manthey CL, Wang S, Rosenzweig B, Bray J, Delaney J, Cole CN, Chan-Hui PY, Mantlo N, Lichenstein HS, Zukowski M, Yao Z. Molecular cloning and characterization of a novel p38 mitogen-activated protein kinase. J Biol Chem 1997;272:23668–74.
[7] Moriguchi T, Toyoshima F, Masuyama N, Hanafusa H, Gotoh Y, Nishida E. A novel SAPK/JNK kinase, MKK7, stimulated by TNF-α and cellular stresses. EMBO J 1997;16:7045–53.
[8] Zu YL, Qi J, Gilchrist A, Fernandez GA, Vazquez-Abad D, Kreutzer DL, Huang CK, Sha'afi RI. p38 mitogen-activated protein kinase activation is required for human neutrophil function triggered by TNF-α or FLMP stimulation. J Immunol 1998;160:1982–9.
[9] Rutault K, Hazzalin CA, Mahadevan LC. Combinations of ERK and p38 MAPK inhibitors ablate tumor necrosis factor-α (TNF-α) mRNA induction: evidence for selective destabilization of TNF-α transcripts. J Biol Chem 2001;276:6666–74.
[10] Meister A. Glutathione metabolism and its selective modification. J Biol Chem 1988;263:17205–8.
[11] Hayes JD, McLellan LI. Glutathione and glutathione-dependent enzymes represent a coordinately regulated defense against oxidative stress. Free Rad Res 1999;31:273–300.
[12] Rahman I. Inflammation and the regulation of glutathione level in lung epithelial cells. Antiox-Redox Signal 1999;1:425–47.
[13] Haddad JJ, Land SC. O_2-evoked regulation of HIF-1α and NF-κB in perinatal lung epithelium requires glutathione biosynthesis. Am J Physiol Lung Cell Mol Physiol 2000;278:L492–503.
[14] Haddad JJ, Olver RE, Land SC. Antioxidant/pro-oxidant equilibrium regulates HIF-1α and NF-κB redox sensitivity: evidence for inhibition by glutathione oxidation in alveolar epithelial cells. J Biol Chem 2000;275:21130–9.
[15] Rahman I. Regulation of nuclear factor-κB, activator protein-1, and glutathione levels by tumor necrosis factor-α and dexamethasone in alveolar epithelial cells. Biochem Pharmacol 2000;60:1041–9.
[16] Dröge W, Schulze-Osthoff K, Mihm S, Galter D, Schenk H, Eck HP, Roth S, Gmunder H. Functions of glutathione and glutathione disulfide in immunology and immunopathology. FASEB J 1994;8:1131–8.
[17] Thompson AB, Robbins RA, Romberger DJ. Immunological functions of the pulmonary epithelium. Eur Respir J 1985;8:127–49.
[18] Rovin BH, Dickerson JA, Tan LC, Fassler J. Modulation of IL-1-induced chemokine expression in human mesangial cells through alterations in redox status. Cytokine 1997;9:178–86.
[19] Jeannin P, Delneste Y, Lecoanet-Henchoz S, Gauchat JF, Life P, Holmes D, Bonnefoy JY. Thiols decrease human interleukin (IL)-4 production and IL-4-induced immunoglobulin synthesis. J Exp Med 1995;182:1785–92.
[20] Gosset P, Wallaert B, Tonnel AB, Fourneau C. Thiol regulation of the production of TNF-α, IL-6 and IL-8 by human alveolar macrophages. Eur Respir J 1999;14:98–105.
[21] Neuschwander-Tetri BA, Bellezzo JM, Brittonm RS, Bacon BR, Fox ES. Thiol regulation of endotoxin-induced release of tumor necrosis factor α from isolated rat Kupffer cells. Biochem J 1996;320:1005–10.
[22] Matsumoto K, Hashimoto S, Gon Y, Nakayama T, Horie T. *N*-Acetylcysteine inhibits IL-1α-induced IL-8 secretion by human bronchial epithelial cells. Respir Med 1998;92:512–5.
[23] Reimund J-M, Allison AC, Muller CD, Dumont S, Kenney JS, Baumann R, Duclos B, Poindron P. Antioxidants inhibit the *in vitro* production of inflammatory cytokines in Crohn's disease and ulcerative colitis. Eur J Clin Invest 1998;28:145–50.
[24] Barrett EG, Johnston C, Oberdörster G, Finkelstein JN. Antioxidant treatment attenuates cytokine and chemokine levels in murine macrophages following silica exposure. Toxicol Appl Pharmacol 1999;158:211–20.
[25] Haddad JJ, Safieh-Garabedian B, Saadé NE, Kanaan SA, Land SC. Chemioxyexcitation (ΔpO_2/ROS)-dependent release of IL-1β, IL-6 and TNF-α: Evidence of cytokines as oxygen sensitive mediators in the alveolar epithelium. Cytokine 2001;13:138–47.
[26] Haddad JJ, Safieh-Garabedian B, Saadé NE, Land SC. Thiol regulation of pro-inflammatory cytokines reveals a novel immunopharmacological potential of glutathione in the alveolar epithelium. J Pharmacol Exp Therap 2001;296:996–1005.

[27] Pena LR, Hill BB, McClain CJ. Treatment with glutathione precursor decreases cytokine activity. J Parenter Enteral Nutr 1999;23:1–6.
[28] Bernard GR. *N*-Acetyl-L-cysteine in experimental and clinical acute lung injury. Am J Med 1991;91(3C):54S–9S.
[29] Tsuji F, Miyake Y, Aono H, Kawashima Y, Mita S. Effects of bucillamine and *N*-acetyl-L-cysteine on cytokine production and collagen-induced arthritis (CIA). Clin Exp Immunol 1999;115:26–31.
[30] Hashimoto S, Gon Y, Matsumoto K, Takeshita I, Horie T. *N*-Acetylcysteine attenuates TNF-α-induced p38 MAP kinase activation and p38 MAP kinase-mediated IL-8 production by human pulmonary vascular endothelial cells. Br J Pharmacol 2001;132:270–6.
[31] Griffith OW, Meister A. Potent and specific inhibition of glutathione synthesis by buthionine sulfoximine (*S-n*-butyl homocysteine sulfoximine). J Biol Chem 1979;254:7558–60.
[32] Hashimoto S, Matsumoto K, Gon Y, Furuichi S, Maruoka S, Takeshita I, Hirota K, Yodoi J, Horie T. Thioredoxin negatively regulates p38 MAP kinase activation and IL-6 production by tumor necrosis factor-α. Biochem Biophys Res Commun 1999;258:443–7.
[33] Hashimoto S, Matsumoto K, Gon Y, Maruoka S, Takeshita I, Hayashi S, Koura K, Kujime K, Horie T. p38 mitogen-activated protein kinase regulates IL-8 expression in human pulmonary vascular endothelial cells. Eur Respir J 1999;13:1357–64.
[34] Ridley SH, Sarsfield SJ, Lee JC, Bigg HF, Cawston TE, Taylor DJ, Dewitt DL, Saklatvala J. Actions of IL-1 are selectively controlled by p38 mitogen-activated protein kinase: regulation of prostaglandin H synthase-2, metalloproteinases, and IL-6 at different levels. J Immunol 1997;158:3165–73.
[35] Nick JA, Avdi NJ, Young SK, Lehman LA, McDonald PP, Frasch SC, Billstrom MA, Henson PM, Johnson GL, Worthen GS. Selective activation and functional significance of p38α mitogen-activated protein kinase in lipopolysaccharide-stimulated neutrophils. J Clin Investig 1999;103:851–8.
[36] Partrick DA, Moore EE, Offner PJ, Meldrum DR, Tamura DY, Johnson JL, Silliman CC. Maximal human neutrophil priming for superoxide production and elastase release requires p38 mitogen-activated protein kinase activation. Arch Surg 2000;135:219–25.
[37] Haddad JJ, Land SC. The differential expression of apoptosis factors in the alveolar epithelium is redox sensitive and requires NF-κB (RelA)-selective targeting. Biochem Biophys Res Commun 2000; 271:257–67.
[38] Haddad JJ, Lauterbach R, Saadé NE, Safieh-Garabedian B, Land SC. α-Melanocyte-related tripeptide, Lys-D-Pro-Val, ameliorates endotoxin-induced nuclear factor κB translocation and activation: evidence for involvement of an interleukin-$1\beta^{193-195}$ receptor antagonism in the alveolar epithelium. Biochem J 2001;355:29–38.
[39] Safieh-Garabedian B, Kanaan SA, Haddad JJ, Abou Jaoude P, Jabbur SJ, Saadé NE. Involvement of interleukin-1β, nerve growth factor and prostaglandin E_2 in endotoxin-induced localized inflammatory hyperalgesia. Br J Pharmacol 1997;121:1619–26.
[40] Pittet JF, Mackersie RC, Martin TR, Matthay MA. Biological markers of acute lung injury: prognostic and pathogenetic significance. Am J Respir Crit Care Med 1997;155:1187–205.
[41] Haddad JJ, Choudhary KK, Land SC. The *ex vivo* differential expression of apoptosis signalling cofactors in the developing lung: essential role of oxygenation during the transition from placental to pulmonary-based respiration. Biochem Biophys Res Commun 2001; 281:311–6.
[42] Rietschel ET, Kirikae T, Schade U, Mamat U, Schmidt G, Loppnow H, Ulmer A, Zahringer U, Seydel U, Padova F, Schrier M, Brade H. Bacterial endotoxin: molecular relationships of structure to activity and function. FASEB J 1994;8:217–25.
[43] Haskó G, Kuhel DG, Németh ZH, Mabley JG, Stachlewitz RF, Virág L, Lohinai Z, Southan GJ, Salzman AL, Szabó C. Inosine inhibits inflammatory cytokine production by a post-transcriptional mechanism and protects against endotoxin-induced shock. J Immunol 2000;164:1013–9.
[44] Haskó G, Szabó C, Németh ZH, Salzman AL, Sylvester Vizi E. Suppression of IL-12 production by phosphodiesterase inhibition in murine endotoxemia is IL-10 independent. Eur J Immunol 1998;28: 468–72.
[45] Doherty AM. Phosphodiesterase 4 inhibitors as novel anti-inflammatory agents. Curr Opin Chem Biol 1999;3:466–73.
[46] Visser J, Van Boxel-Dezaire A, Methorst D, Brunt T, Ronald De Kloet E, Nagelkerken L. Differential regulation of interleukin-10 (IL-10) and IL-12 by glucocorticoids *in vitro*. Blood 1998;91: 4255–64.
[47] Fukuda T, Sumichika H, Murata M, Hanano T, Adachi K, Hisadome M. A novel dual regulator of tumor necrosis factor-α and interleukin-10 protects mice from endotoxin-induced shock. Eur J Pharmacol 2000;391:317–20.
[48] Haddad JJ, Safieh-Garabedian B, Land NE, Land SC. The biphasic immnoregulation of pyrimidylpiperazine (Y-40138) is IL-10 sensitive and requires NF-κB targeting in the alveolar epithelium. Br J Pharmacol 2001;133:49–60.
[49] Hanano T, Adachi K, Aoki Y, Morimoto H, Naka Y, Hisadome M, Fukuda T, Sumichika H. Novel DMARDs on the basis of a new concept of dual cytokine regulation, TNF-α suppression and IL-10 augmentation. Bioorg Med Chem Lett 2000;10:881–4.
[50] Hisadome M, Fukuda T, Sumichika H, Hanano T, Adachi K. A novel anti-rheumatic drug suppresses tumor necrosis factor-α and augments interleukin-10 in adjuvant arthritic rats. Eur J Pharmacol 2000;409: 331–5.
[51] Han J, Lee JD, Bibbs L, Ulevitch RJ. A MAP kinase targeted by endotoxin and hyperosmolarity in mammalian cells. Science 1994;265:808–11.
[52] Rouse J, Cohen P, Trigon S, Morange M, Alonso-Llamazares A, Zamanillo D, Hunt T, Nebreda AR. A novel kinase cascade triggered by stress and heat shock stimulates MAPKAP kinase-2 and phosphorylation of the small heat shock proteins. Cell 1994;78: 1027–37.
[53] Baldassare JJ, Bi Y, Bellone CJ. The role of p38 mitogen-activated protein kinase in IL-1β transcription. J Immunol 1999;162:5367–73.
[54] Cano E, Mahadevan LC. Parallel signal processing among mammalian MAPKs. Trends Biochem Sci 1995;20:117–22.
[55] Hudson LD, Milberg JA, Anardi D, Maunder RJ. Clinical risks for the development of the acute respiratory distress syndrome. Am J Respir Crit Care Med 1995;151:293–301.
[56] Vandenabeele P, Declercq W, Beyaert R, Fiers W. Two tumor necrosis factor receptors: structure and function. Trends Cell Biol 1995;5:392–9.
[57] Kotlyarov A, Neininger A, Schubert C, Eckert R, Birchmeier C, Volk HD, Gaestel M. MAPKAP kinase 2 is essential for LPS-induced TNF-α biosynthesis. Nature Cell Biol 1999;1:94–7.
[58] De Keulenaer GW, Ushio-Fukai M, Yin Qiqin Chung AB, Lyons PR, Ishizaka N, Rengarajan K, Taylor WR, Alexander RW, Griendling KK. Convergence of redox-sensitive and mitogen-activated protein kinase signaling pathways in tumor necrosis factor-α-mediated monocyte chemoattractant protein-1 induction in vascular smooth muscle cells. Arterioscler Thromb Vasc Biol 2000;20:385–91.
[59] Kang KW, Ryu JH, Kim SG. The essential role of phosphatidylinositol 3-kinase and of p38 mitogen-activated protein kinase activation in the antioxidant response element-mediated rGSTA2 induction by decreased glutathione in H4IIE cells. Mol Pharmacol 2000;58: 1017–25.
[60] Chan ED, Riches DWH, White CW. Redox paradox: effect of *N*-acetylcysteine and serum on oxidation–reduction-sensitive mitogen-activated protein kinase signaling pathways. Am J Respir Cell Mol Biol 2001;24:627–32.
[61] Wright SD, Ramos RA, Tobias PS, Ulevitch RJ, Mathison JC. CD14, a receptor for complexes of lipopolysaccharide (LPS) and LPS binding protein. Science 1990;249:1431–3.
[62] Mercurio F, Manning AM. Multiple signals converging on NF-κB. Curr Opin Cell Biol 1999;11:226–32.

[63] Widmann C, Gibson S, Jarpe MB, Johnson GL. Mitogen-activated protein kinase: conservation of a three-kinase module from yeast to human. Physiol Rev 1999;79:143–80.
[64] Griego SD, Weston CB, Adams JL, Tal-Singer R, Dillon SB. Role of p38 mitogen-activated protein kinase in rhinovirus-induced cytokine production by bronchial epithelial cells. J Immunol 2000;165:5211–20.
[65] Foey AD, Parry SL, Williams LM, Feldmann M, Foxwell BMJ, Brennan FM. Regulation of monocyte IL-10 synthesis by endogenous IL-1 and TNF-α: role of the p38 and p42/44 mitogen-activated protein kinases. J Immunol 1998;160:920–8.
[66] De AK, Kodys KM, Yeh BS, Miller-Graziano C. Exaggerated human monocyte IL-10 concomitant to minimal TNF-α induction by heat-shock protein 27 (Hsp27) suggests Hsp27 is primarily an anti-inflammatory stimulus. J Immunol 2000;165:3951–8.
[67] Yamakawa T, Eguchi S, Matsumoto T, Yamakawa Y, Numaguchi K, Miyata I, Reynolds CM, Motley ED, Inagami T. Intracellular signalling in rat cultured vascular smooth muscle cells: roles of nuclear factor-κB and p38 mitogen-activated protein kinase on tumor necrosis factor-α production. Endocrinology 1999;140:3562–73.
[68] Ballard-Croft C, White DJ, Maass DL, Hybki DP, Horton JW. Role of p38 mitogen-activated kinase in cardiac myocyte secretion of the inflammatory cytokine TNF-α. Am J Physiol Heart Circ Physiol 2001;280:H1970–81.
[69] Scherle PA, Jones EA, Favata MF, Daulerio AJ, Covington MB, Nurnberg SA, Magolda RL, Trzaskos JM. Inhibition of MAP kinase kinase prevents cytokine and prostaglandin E_2 production in lipopolysaccharide-stimulated monocytes. J Immunol 1998;161:5681–6.
[70] Aruoma OI, Halliwell B, Hoey BM, Beutler J. The antioxidant action of *N*-acetyl-L-cysteine: its reaction with hydrogen peroxide, hydroxyl radical, superoxide, and hypochloric acid. Free Rad Biol Med 1989;6:593–7.
[71] Natoli G, Costanzo A, Ianni A, Templeton DJ, Woodgett JR, Balsano C, Levrero M. Activation of SAPK/JNK by TNF receptor I through a non-cytotoxic TRAF2-dependent pathway. Science 1997;275:200–3.
[72] Saitoh M, Nishitoh H, Fuji M, Takeda K, Tobium K, Sawada Y, Kawabata M, Miyazono K, Ichijo H. Mammalian thioredoxin is a direct inhibitor of apoptosis signal regulating kinase (ASK)-1. EMBO J 1998;17:2596–606.